Electrostatic micromachine scanning mirror for optical coherence tomography

J. M. Zara

Department of Electrical and Computer Engineering, George Washington University, Washington, D.C. 20052

S. Yazdanfar, K. D. Rao, J. A. Izatt, and S. W. Smith

Department of Biomedical Engineering, Duke University, Durham, North Carolina 27708

Received September 27, 2002

Compact electrostatic micromirror structures for use in the scanning arm of an optical coherence tomography (OCT) system are described. These devices consist of millimeter-scale mirrors resting upon micrometer-scale polyimide hinges that are tilted by a linear micromachine actuator, the integrated force array (IFA). The IFA is a network of deformable capacitor cells that electrostatically contract with an applied voltage. The support structures, hinges, and actuators are fabricated by photolithography from polyimide-upon-silicon wafers. These devices were inserted into the scanning arm of an experimental OCT imaging system to produce *in vitro* and *in vivo* images at frame rates of 4 to 8 Hz. © 2003 Optical Society of America

OCIS codes: 110.4500, 120.5800, 170.3880.

Optical coherence tomography (OCT) is an optical imaging technique that is analogous to B-mode medical ultrasound and uses infrared light to interrogate an imaging target. Light reflected from scattering sites within a sample is localized in depth by low-coherence interferometry. Scanning a reference delay line while recording the interferometric detector response creates a map of reflectivity relative to optical depth. Two-dimensional images are made from sequential longitudinal image lines of backscatter versus distance into the sample. OCT produces tomographic images of subsurface microscopic structures with a resolution of 10 μm or less.[1] Whereas OCT images exhibit high spatial resolution, penetration depths are limited to 1–3 mm because of the high level of scattering of infrared light in biological tissues.[2]

OCT has shown promise in applications including imaging of the eye and in intravascular and gastrointestinal imaging with endoscopic and catheter probes.[3,4] A crucial component of the OCT system is the method by which the optical beam is scanned across the target to create a two-dimensional image. For endoscopic and intravascular applications, limited space in the probe restricts the actuation methods available for use. In this Letter we demonstrate a compact microelectromechanical-system- (MEMS-) based scanning element for potential use in catheter- and endoscope-based OCT imaging systems.

One endoscopic OCT system design used in clinical trials includes a spinning reflective element to scan the infrared beam across the tissue in a circular side-scanning configuration.[3,5] This scanning arrangement allows the imaging probe to view only targets that are directly adjacent to the probe. A sector-scanning probe would enable images to be created in a large sector to the side or the front of the probe to guide interventional procedures conducted with instruments that are introduced concurrently with the imaging device. Several OCT probes have been developed that image in a noncircumferential scan geometry. These include probes that use piezoelectric bimorphs to scan the imaging fiber,[6] probes that use thermoelectric actuators to swing a scanning mirror,[7] and a probe that uses a linear-scanning galvanometer to move the optics in a catheter probe.[8] Whereas these probes have demonstrated success, the devices that we are developing may have certain advantages over existing technologies. These include low power consumption of the MEMS actuator, low costs because the key components are made with microfabrication, and the potential for large scan displacements for certain applications.

These MEMS scanning devices were originally fabricated for applications in high-frequency ultrasound and industrial optical beam steering.[9–11] For optical beam steering applications, these devices consist of gold-plated silicon mirrors mounted upon polyimide tables that pivot on 3-μm-thick polyimide torsion hinges. A linear actuator on the side of the mirror table contracts in length and pulls on an attachment flap to tilt

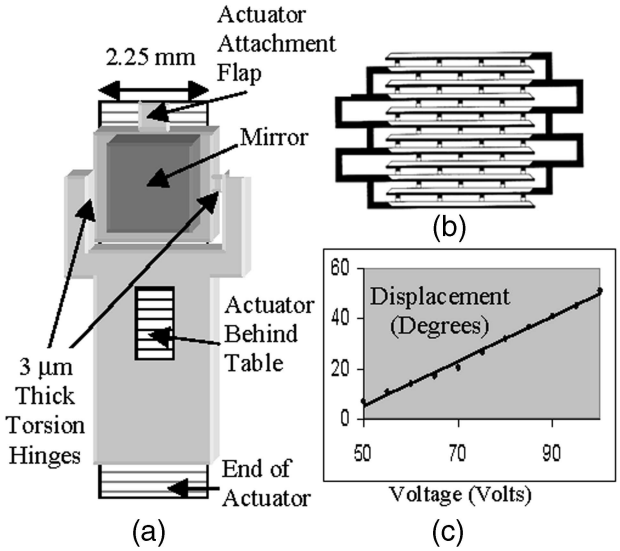

Fig. 1. Schematics of (a) the fabricated scanner and (b) a portion of the cells in the IFA electrostatic MEMS actuator. (c) Plot of optical displacement versus drive voltage for this MEMS scanner.

0146-9592/03/080628-03$15.00/0

the mirror and scan the reflected beam. Figure 1(a) is a schematic showing a front view of these optical scanning devices with the linear actuator shown behind the mirror support structure.

The linear MEMS actuator used to tilt the mirror, the integrated force array (IFA), is a network of hundreds of thousands of micrometer-scale deformable capacitors. The capacitive cells contract because of the presence of electrostatic forces produced by a differential voltage applied across the capacitor electrodes. Figure 1(b) is a schematic of a portion of the cell network of the IFA. The small scale of the cells allows these devices to utilize the short-range electrostatic forces effectively by reducing the distance between the electrodes and also by allowing for large numbers of cells to contribute to forces and displacements. The IFA was described previously.[12,13] These devices are 1 or 3 mm wide and 1 cm long and include as many as 500,000 capacitive cells in three columns. They have been shown to produce strains of as much as 20% and forces up to 13 dyne with applied voltages of ± 65 V. Also, because the capacitive cells draw current only when they are contracting, power consumption is very low; we have measured the power consumption to be less than 2 mW.

The mirror assemblies were fabricated by a two-layer process upon 12.7-cm silicon wafers. To form the thin hinge layer, a 3-μm layer of polyimide (PI-2723, HD Microsystems, Wilmington, Del.) was spun onto the wafer and then patterned. The thicker supports and tables were made from a 30-μm-thick patterned polyimide layer (Durimide, Arch Chemicals, Norwalk, Conn.). A sacrificial silicon oxide layer was deposited upon the wafer before processing to release the polyimide structures from the wafer and was then etched away by hydrofluoric acid. The table structures that were fabricated measured 2 mm by 2.25 mm wide. The torsion hinges upon which the tables tilt were 3 μm thick, 250 μm long, and 135 μm wide. After the devices were lifted off the silicon wafers, gold-coated silicon mirrors 1.5 mm on a side were bonded to the tables. The final step in assembly was to attach the IFA actuator to the attachment flap on the table. Figure 1(c) is a plot of the measured optical displacement of this MEMS optical scanner as a function of drive voltage that shows that the motion of the scanner is relatively linear.

Figure 2 contains a photograph of the scanning device as used and a schematic of a proposed endoscopic probe tip. For this MEMS mirror to be used in endoscopic studies it is necessary to encase the probe tip to protect it from the environment. Packaging of the MEMS device presents a complicated design problem. Major issues include miniaturizing the optics and designing and fabricating an encasement sheath to protect the fragile MEMS actuator while providing room for the mirror to tilt. It is also essential to have an optical window for the imaging beam to pass through with minimal signal loss and distortion. Figure 2(b) shows a graded-index (GRIN) lens and a micro right-angle prism and the encasement sheath and optical window under development. We have specified and obtained the optics necessary for the endoscopic design and are currently working on an encasement tip to increase the robustness of the sensitive scanner.

The probe was incorporated into the lateral scanning arm of the experimental high-speed OCT system shown in Fig. 3.[5] The system used a superluminescent diode as a light source with a FWHM bandwidth of 28 nm and a center wavelength of 1290 nm, resulting in a free-space coherence length of 20 μm. The reference arm consisted of a Fourier-domain rapid scanning optical delay line based on a resonant scanner oscillating at a rate of 2 kHz, and images were acquired at frame rates of 4–8 frames/s. Both the forward and the reverse scans of the delay line were used, resulting in acquisition rates of 4000 lines/s. To incorporate the MEMS scanner into the OCT system, the beam was collimated onto the scanning mirror at a 45° angle. A lens ($f = 50.2$ mm) was placed one focal length away from the scanner, and the target was one focal length away from the lens. Approximately 3 mW of optical power was delivered to the sample.

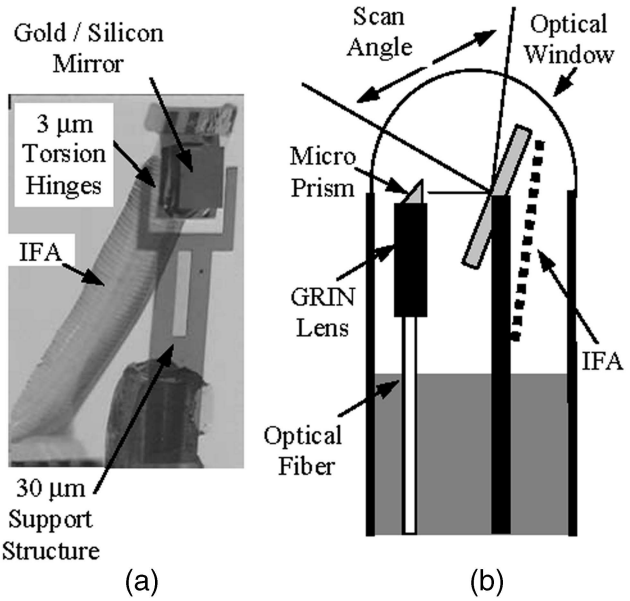

Fig. 2. MEMS scanning device: (a) photograph of the device, (b) schematic of the scanner encased in the proposed endoscopic probe.

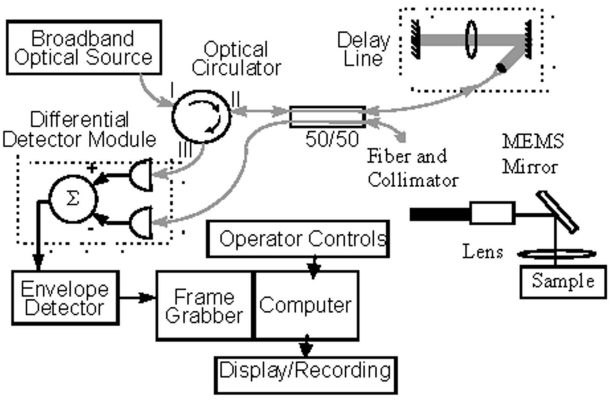

Fig. 3. Schematic of the OCT system with the electrostatic MEMS actuator as the scanning arm.

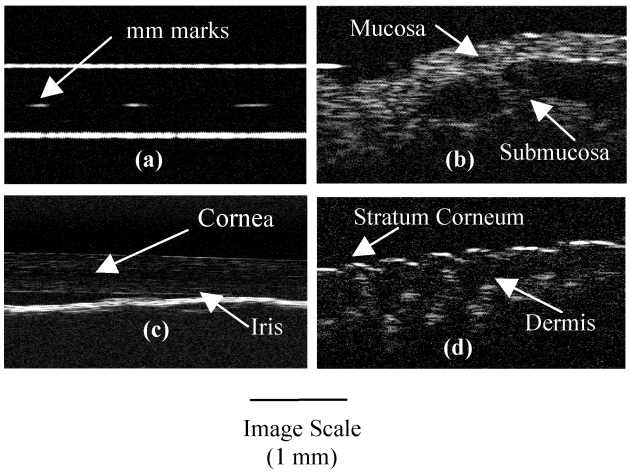

Fig. 4. Images obtained with an OCT system incorporating an electrostatic MEMS actuator: (a) clear plastic ruler, showing the top and bottom surfaces and millimeter demarcations; (b) *in vitro* porcine colon tissue; (c) *in vitro* porcine eyeball, showing cornea and iris; (d) *in vivo* dermal ridges of the underside of a human index finger.

The MEMS actuator was powered with voltage control signals from an arbitrary waveform generator and was scanned at a frequency of 4 Hz. Figure 4 contains still images of several structures, both *in vivo* and *in vitro*, obtained with the probe used as the scanning arm of the OCT system. Figure 4(a) is a scan of a clear plastic ruler, demonstrating the flatness of the scan and the scan range of 3 mm. Figure 4(b) is an *in vitro* scan of the lining of an excised porcine colon. Figure 4(c) is an *in vitro* scan of a porcine eye, showing the cornea and iris. Finally, Fig. 4(d) is an *in vivo* image of the underside of a human finger, showing the dermal ridges. The images in Fig. 4 have lateral scan ranges of 3–5 mm, but these scanners have the potential to produce much larger scan ranges. We have demonstrated optical scan angles of more than 140° near the resonant frequencies of the scanners[11] and have collected images with scan ranges of 8–12 mm but with diminished image quality because of interface problems between the OCT system and the probe.

Figure 4(a) demonstrates some distortion in the images, with the spacing between the millimeter marks increasing across the scan. Figure 2(c) demonstrates that the scan angle as a function of drive voltage is relatively linear, so we believe that this distortion is a function not of the scanner's motion but of the scanner's speed. This distortion results from the scanner's slowing down as it changes direction while the imaging system is grabbing data lines at a constant rate. This distortion is often eliminated in mechanical scanning systems by truncation of the images near the ends of the scan, which reduces the usable scan range. Another potential solution would be to monitor the current position of the scanning mirror and adjust the display to correlate with the scanning position. One potential method being investigated is to monitor the capacitance of the MEMS actuator to determine its position and use feedback to adjust the display in the scan.

In this Letter we have presented the design, fabrication, and integration of a new type of MEMS-driven mirror device into the scanning arm of a real-time OCT imaging system. We have demonstrated that these devices can be integrated into existing OCT systems for imaging purposes. Preliminary experimentation has shown the feasibility of the compact optical scanner that we have developed for OCT applications, but the existing scanner needs to be further modified for endoscopic applications, as was discussed above. We are also developing processes that will enable the entire device to be fabricated upon the same silicon wafer, therefore facilitating assembly and reducing the cost of the probes.

We gratefully acknowledge the technical assistance of L. Thrane and B. Wolf. This research was supported in part by National Institutes of Health grants HL-58754, HL-64962, and EY-13015. S. Yazdanfar was also with the Department of Biomedical Engineering, Case Western Reserve University, Cleveland, Ohio, 44106. J. Zara's e-mail address is jzara@gwu.edu.

References

1. A. F. Fercher, J. Biomed. Opt. **1,** 157 (1996).
2. J. G. Fujimoto, M. E. Brezinski, G. J. Tearney, S. A. Boppart, B. Bouma, M. R. Hee, J. F. Southern, and E. A. Swanson, Nature Med. **1,** 970 (1995).
3. G. J. Tearney, M. E. Brezinski, B. E. Bouma, S. A. Boppart, C. Pitris, J. F. Southern, and J. G. Fujimoto, Science **276,** 2037 (1997).
4. A. M. Sergeev, V. M. Gelikonov, G. V. Gelikonov, F. I. Feldchtein, R. V. Kuranov, N. D. Gladkova, N. M. Shakhova, L. B. Snopova, A. V. Shakhov, I. A. Kuznetzova, A. N. Denisenko, V. V. Pochinko, Yu. P. Chumakov, and O. S. Streltzova, Opt. Express **13,** 432 (1997), http://www.opticsexpress.org.
5. A. M. Rollins, R. Ung-arunyawee, A. Chak, R. C. K. Wong, K. Kobayashi, M. V. Sivak, Jr., and J. A. Izatt, Opt. Lett. **24,** 1358 (1999).
6. S. A. Boppart, B. E. Bouma, C. Pitris, G. J. Tearney, and J. G. Fujimoto, Opt. Lett. **22,** 1618 (1997).
7. Y. Pan, H. Xie, and G. K. Fedder, Opt. Lett. **26,** 1966 (2001).
8. B. E. Bouma and G. J. Tearney, Opt. Lett. **24,** 531 (1999).
9. J. M. Zara, S. M. Bobbio, S. Goodwin-Johansson, and S. W. Smith, IEEE Trans. Ultrason. Ferroelectr. Freq. Control **47,** 984 (2000).
10. J. M. Zara and S. W. Smith, IEEE Trans. Ultrason. Ferroelectr. Freq. Control **49,** 947 (2002).
11. J. M. Zara and S. W. Smith, Sens. Actuators A **102,** 176 (2002).
12. J. Jacobson, S. Goodwin-Johansson, S. Bobbio, C. Bartlett, and L. Yadon, IEEE J. Microelectrical Systems **4,** 139 (1995).
13. S. Bobbio, S. Smith, S. Goodwin-Johansson, R. Fair, T. DuBois, F. Tranjan, J. Hudak, R. Gupta, and H. Makki, Proc. SPIE **3046,** 248 (1997).